Instruments and Experimental Techniques, Vol. 42, No. 6, 1999, pp. 827–834. Translated from Pribory i Tekhnika Eksperimenta, No. 6, 1999, pp. 104–111.
Original Russian Text Copyright © 1999 by Tour'yanski, Pirshin.

GENERAL EXPERIMENTAL TECHNIQUES

X-Ray Refractometry of Surface Layers

A. G. Tour'yanski and I. V. Pirshin

Lebedev Physical Institute, Russian Academy of Sciences, Leninskii pr. 53, Moscow, 117924 Russia

Received March 5, 1999

Abstract—An X-ray refractometry method with a radiation wavelength of ~0.1 nm is described. A probing beam is directed to a surface under study from the inside through a side cleaved face of a sample or in the opposite direction. The method provides high reliability of measurements and allows small-area analyses. This makes it possible to use it in cases where a device structure is formed on part of a sample and, moreover, sharply decreasing requirements are imposed on the flatness of the sample surface. Results of the measurement of parameters of surface layers for GaAs single crystals and multilayer heterostructures based on Ge_xSi_{1-x}/Si are presented.

INTRODUCTION

In our previous paper [1], we described a new scheme for an X-ray reflectometer with two working wavelengths and presented various examples of angular-dependent reflectivity measurements. Here, we analyze the feasibility of application of the scheme proposed to the study of parameters of surface layers, with the help of X-ray refractometry.

The first measurements of the refraction of X-rays with a wavelength of ~0.1 nm were made by Hartley [2] when studying different orders of reflection from crystals. Results of the measurement of X-ray refraction on samples of amorphous materials were presented for the first time in [3]. The measurement accuracy was substantially improved by using a version of the scheme of a two-crystal spectrometer for the measurement of the angular shift of the refracted beam with respect to the reference one [4, 5]. The results obtained in [2–5] were important as a verification of the validity of the theory of electromagnetic waves in frequency ranges exceeding optical frequencies by 3–4 orders of magnitude. However, they were of little practical importance, i.e., as a measurement technique. Firstly, the X-ray optical parameters of a material could be rather easily obtained from the angular dependences of reflectivity in the region of total external reflection [6, 7]. Secondly, specially manufactured prisms with polished faces forming an obtuse angle were used in the measurements in order to provide a double passage of radiation through an interface at small grazing angles.

It should be noted that interest in the problem of practical use of the refraction of X-ray radiation with energy greater than 20 keV has been rekindled recently. However, this is associated with the feasibility of production of focusing systems [8] and obtaining phase contrast by radioscopy of objects [9, 10] and not with metrology.

When working with samples of polished wafers produced from single crystals by cleaving along the cleavage plane, or an arbitrary line specified by a scriber, we found no deformations along the edge of a fracture that caused deviation from flatness. Moreover, the quality of the cleaved surface had no noticeable effect on the results of measurements of the refraction angle in the case of successive transmission of a beam through a cleaved surface and an optically polished one. This means that a wide class of objects used in physical experiments and practice requires no special preparation for refractometric measurements. Therefore, the main problem in our case is to evaluate the analytical possibilities of the method and interpret the results obtained when using it.

Substantiation of the Method

If a plane electromagnetic wave, polarized perpendicular to the plane of incidence, falls on the interface between two uniform media, the angular dependence of the ratio of amplitudes of the reflected (E_s) and incident (E_{os}) waves is given by the Fresnel formula [11]

$$\frac{E_s}{E_{os}} = \frac{\sin\varphi_1 - n\sin\varphi_2}{\sin\varphi_1 + n\sin\varphi_2}, \quad (1)$$

where φ_1 and φ_2 are the angle of incidence and the refraction angle in the first and second media, respectively, which are measured from the normal, and $n = n_2/n_1$ is the relative refractive index representing, in the wavelength range under consideration, a complex quantity.

Let us introduce a change to the grazing angles $\theta_1 = \pi/2 - \varphi_1$ and $\theta_2 = \pi/2 - \varphi_2$, which are commonly used in X-ray refractometry. They are measured from the interface to the directions of propagation of the incident and refracted waves, respectively. We represent the refractive index of the sample material in the form $n_1 = 1 - \delta - i\beta$ and assume that the second medium is vacuum (air); i.e., $n_2 = 1$. We also assume, for definiteness, that radiation enters a sample through a side face at an

0020-4412/99/4206-0827$22.00 © 1999 МАИК "Наука/Interperiodica"

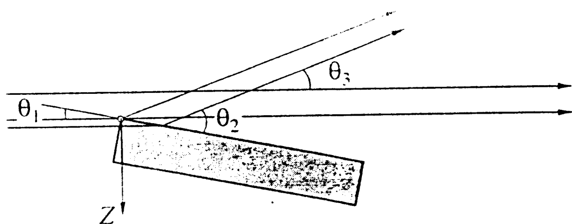

Fig. 1. Geometry of the path of rays in the case of part of the primary beam entering a sample through a side face.

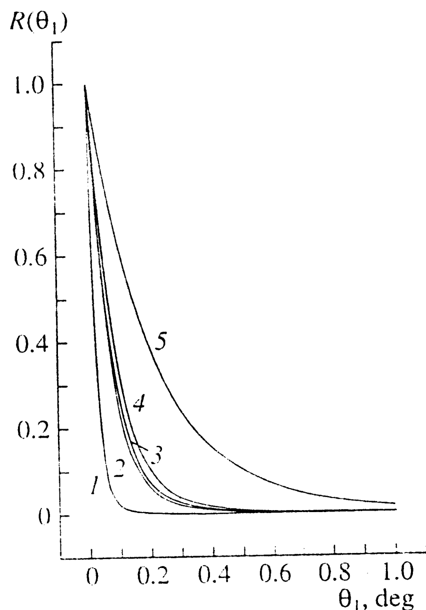

Fig. 2. Calculated angular dependences of the reflectivity of the sample–vacuum interface for the incidence of radiation from inside for different decrements of the refractive index: (1) $\delta \doteq 10^{-6}$, $\beta = 0$; (2) $\delta = 10^{-5}$, $\beta = 0$; (3) $\delta = 10^{-5}$, $\beta = 5 \times 10^{-6}$; (4) $\delta = 10^{-5}$, $\beta = 10^{-5}$; and (5) $\delta = 10^{-4}$, $\beta = 0$.

angle close to $\pi/2$, i.e., without refraction by the interface under consideration and reflection from it (Fig. 1). In view of the law of sines

$$\sin\varphi_1/\sin\varphi_2 = n_2/n_1 = 1/(1-\delta-i\beta) \qquad (2)$$

and the smallness of θ_1, θ_2 and δ, $i\beta$ in comparison with unity, we obtain the following expression for reflectivity:

$$R_s = \left|\frac{E_s}{E_{os}}\right|^2 = \frac{(\theta_1-a)^2+b^2}{(\theta_1+a)^2+b^2}; \qquad (3)$$

$$a^2 = \frac{1}{2}\{[(\theta_1^2+2\delta)^2+4\beta^2]^{1/2}+\theta_1^2+2\delta\}; \qquad (4)$$

$$b^2 = \frac{1}{2}\{[(\theta_1^2+2\delta)^2+4\beta^2]^{1/2}-\theta_1^2-2\delta\}. \qquad (5)$$

formulas (3)–(5) formally differ from the expressions extensively used in the case of total external reflection by the signs in auxiliary variables a and b, which has a substantial effect on the form of the angular dependence of reflectivity $R(\theta_1)$. Figure 2 presents the dependences $R(\theta_1)$ calculated using formula (3) for different values of δ and β. In view of the fact that $\mathbf{E}_s/\mathbf{E}_{os} \cong \mathbf{E}_p/\mathbf{E}_{op}$ for $\theta \le 1°$, where $\mathbf{E}_p$ and $\mathbf{E}_{op}$ are the amplitudes of the reflected and incident waves polarized in the plane of incidence, expressions (3)–(5) describe the angular dependence of reflectivity for an arbitrary polarization.

Deflection Angle of the Primary Beam

In the case of an experiment with geometry of the path of rays shown in Fig. 1, the primary beam is conveniently taken as an angular reference. Because of this it is advantageous to derive an equation for the difference angle $\theta_3 = \theta_2 - \theta_1$, which represents the angle of deviation of the refracted beam from the primary one.

In this case, like in a change from equation (1) to (3), one should use the law of sines. As a result, the deviation angle θ_3 is given by the expression

$$\theta_3 = \theta_2 - \theta_1 = \sqrt{\theta_1^2+2\delta+2i\beta}-\theta_1. \qquad (6)$$

Note that in the previous case, the substitution of a complex angle represented a purely formal procedure, while here, we should estimate the effect of its imaginary part because it is precisely the angles' magnitudes that are measured in experiments on refraction. The calculation of the change of the wavefront direction of the refracted beam by the formulas obtained in metal optics [11] shows that the contribution of the imaginary part of the decrement of n_1 to the angular shift of refracted radiation for $\beta/\delta < 0.1$ is of the order of 0.1%, i.e., negligibly low. The above inequality is valid for $\lambda \sim 0.1$ nm for the majority of materials, and therefore one may use the representation $n_1 = 1 - \delta$ and neglect $2i\beta$ in expression (6). Note that in the case where one calculates the reflectivity $R(\theta_1)$ and the transmittance $T(\theta_1) = 1 - R(\theta_1)$ for the radiation incident on an interface from air, a representation of this kind for n_2 is, generally speaking, incorrect. Figure 3 presents the angular dependences $\theta_3(\theta_1)$ for a number of values of δ in a range of 10^{-4}–10^{-6}. For $\lambda \sim 0.1$ nm, a typical value is $\delta \sim 10^{-5}$. According to (6), the limiting sensitivity to the relative change of δ for angles measured and set with an accuracy of ~1″ can reach in this case ~10^{-3}.

Intensity Calculations

Now let us calculate the intensity of the refracted beam taking into account attenuation in a material on the way from a side face to the interface and reflection from it. Assume that a collimated beam of X-rays with a flux density P_λ for a given spectral line λ is incident

on a side face of a sample in the form of a uniform wafer with plane faces intersecting approximately at a right angle. Let the z-axis be perpendicular to the beam direction and the edge formed by the intersection of the side face and the face being studied, and let the origin of coordinates be coincident with the edge (see Fig. 1). For the beam fragment of width dz that is incident on the side face at the distance z from the origin of coordinates, the path length l in the sample is equal to $z(\tan\theta + (\tan\theta)^{-1})$, where θ is the current grazing angle of the incident beam (θ_1). Consider the region of small angles $\theta << \pi/2$. In this case, the intensity of the beam of cross section wdz that sequentially passed through the side surface at the distance z from the origin of coordinates and the second interface is given by the expression

$$dI(z, \theta) \cong T(\theta)P_\lambda w\exp(-\mu z/\theta)dz, \quad (7)$$

where w is the width of the incident beam in the direction perpendicular to the plane of the figure and μ is the linear attenuation coefficient of the material. By integrating over z and assuming that $\exp(-\mu H/\theta) \longrightarrow 0$ for the sample widths $H \geq 0.1$ mm, which are used, we obtain the following expression for the refracted-beam intensity:

$$I(\theta) \cong T(\theta)P_\lambda w\theta/\mu. \quad (8)$$

In this expression, θ/μ represents the effective thickness h_e of the layer through which the refracted radiation travels.

The table presents the values of h_e in Å calculated for Si, Ge, and GaAs single crystals and polycrystalline Ni for different radiation wavelengths and grazing angles of the primary beam.

One can see that the effective thickness of the layer being analyzed is rather small and can be controlled over a wide range by choosing the radiation wavelength and the range of grazing angles.

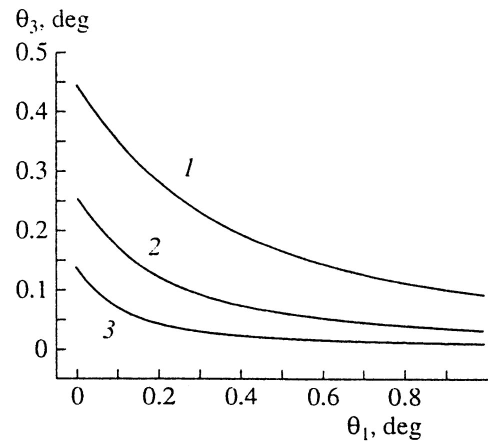

Fig. 3. Dependence of the deviation angle θ_3 on the grazing angle θ_1 for incidence from inside for different values of the real part of the decrement of refractive index δ = (*1*) 3×10^{-5}, (*2*) 10^{-5}, and (*3*) 3×10^{-6}.

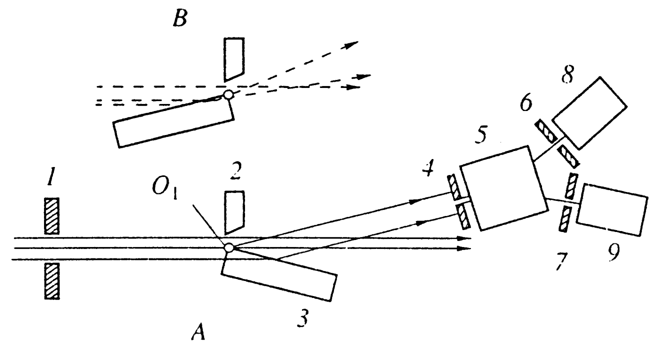

Fig. 4. Schematic diagram of the experimental setup for the measurement of refraction at two characteristic spectral lines: (*1*) output-collimator slit; (*2*) absorbing screen; (*3*) sample; (*4*) receiving slit; (*5*) X-ray beamsplitter; (*6, 7*) collimator slits; and (*8, 9*) scintillation detectors.

EXPERIMENTAL RESULTS

The part of the measuring scheme of a two-wave reflectometer located behind the slit *1* of the output collimator and the path of rays in the measurements of refraction angle are shown in Fig. 4. The setup is described in more detail in [1]. Sample *3* was arranged in one of two positions A or B with respect to the principal goniometer axis O_1. In position A, the O_1 axis was made coincident with the edge formed by the intersection of the polished surface of a sample with the side-cleaved surface facing the radiation source. In position B, the axis was made coincident with the edge formed by the intersection of the polished surface with the cleaved surface facing the receiving slit *4*. Splitter *5* of an X-ray beam on the basis of semitransparent monochromators made of pyrographite [12], collimator slits *6* and *7*, and scintillation detectors *8* and *9* were mounted on a common arm support, which could be rotated about the O_1 axis independently of a sample or in combination with it. Splitter *5* separated, from polychromatic radiation, the characteristic lines CuK_α and CuK_β, which were directed through receiving slits *6* and *7* onto detectors *8* and *9*, respectively. This provided simultaneous data collection at two spectral lines in one cycle of angular scanning. The width of the beam

Values of h_e (in Å) calculated for different materials

	Si		Ge		GaAs		Ni	
λ \ θ_1	0.1°	0.3°	0.1°	0.3°	0.1°	0.3°	0.1°	0.3°
FeK_α	641	1923	180	540	246	738	218	654
CuK_α	1207	3621	460	1380	457	1371	404	1212
CuK_β	1605	4817	607	1822	602	1805	69	208

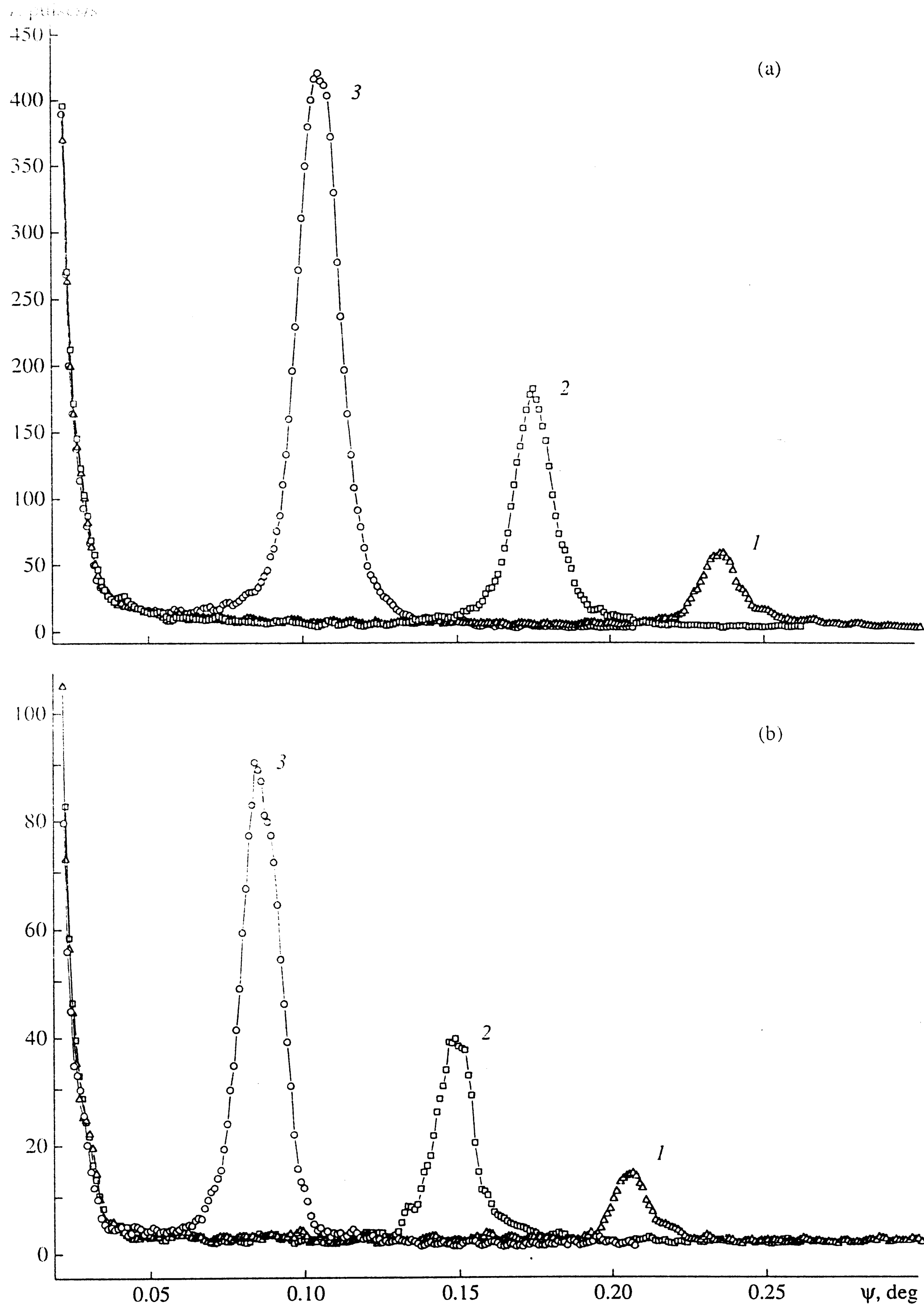

Fig. 5. Angular intensity diagrams for the incidence of radiation from inside onto the surface of a GaAs sample for fixed grazing angles θ_1 = (*1*) 0.09°, (*2*) 0.19°, and (*3*) 0.4° for the (a) CuK_α and (b) CuK_β lines.

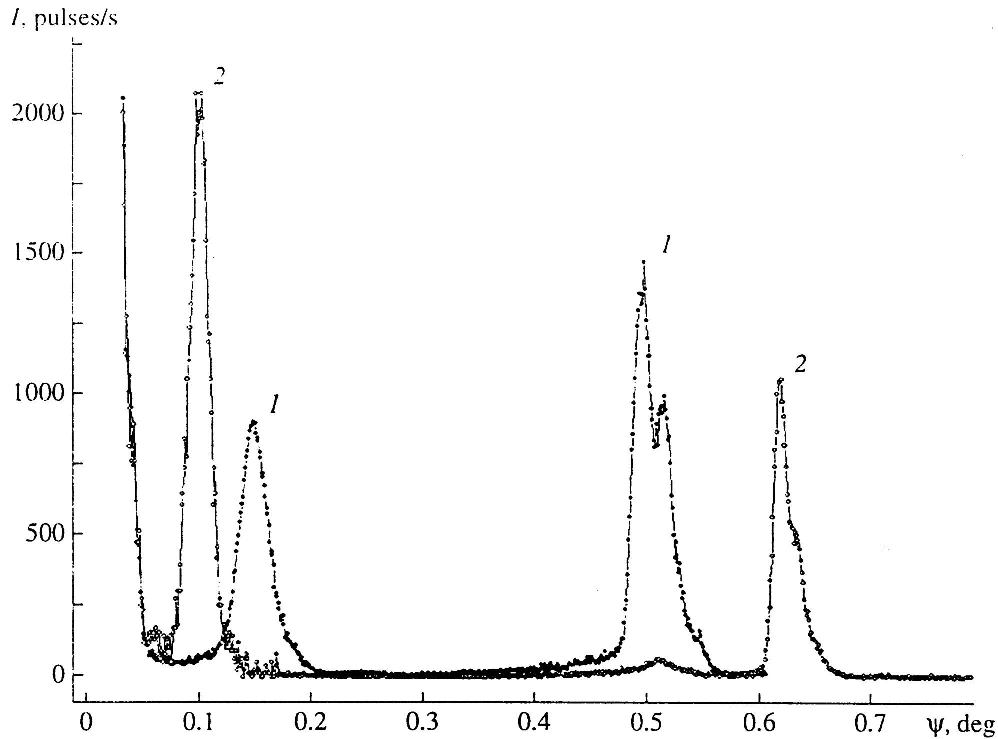

Fig. 6. Angular intensity diagrams for the incidence of radiation from the outside onto the surface of a multilayer Ge–Si heterostructure (position *B* in Fig. 4) for fixed grazing angles θ_1 = (*1*) 0.25° and (2) 0.32°.

traveling above the sample surface is controlled by a micrometric device, which translates an absorbing screen *2*. A typical step of angular scanning over the scale 2θ for the receiving system formed by the elements *4–9* of the scheme was 0.001°.

Prior to measurements, the following conditions of the experiment are established: the position of the polished sample surface corresponding to the zero grazing angle, the ratio of intensities of the spectral lines in the incident beam I_α/I_β, and the X-ray flux densities P_α and P_β. For the optimum adjustment of the two-wave reflectometer, a uniform distribution of the X-ray flux density is provided throughout the width *s* of the spacing between the sample *3* and the absorbing screen *2*. The value of *s* and the distributions of P_α and P_β are determined with a high accuracy by obstructing the direct beam with uniformly rotating sample. If a wide receiving slit *4* is arranged on the axis of the direct X-ray beam, *b* is the sample size in the direction of the beam, θ' and θ'' are the angular positions of a sample corresponding to the initial and final moments of beam obstruction, we have $s = b\sin(\theta'' - \theta') \approx b(\theta'' - \theta')$, and $P_\alpha = I_\alpha/(sw)$, $P_\beta = P_\alpha I_\beta/I_\alpha$, where *w* is the beam width in the direction perpendicular to the plane of the figure for the beam incident on a sample.

Figure 5 shows the angular diagrams of intensity for a GaAs sample of size 6 × 8 mm arranged in position *A*. The diagrams were obtained by angular scanning with the help of the recording system *4–9* for a number of fixed grazing angles for the radiation incident from the inside. In accordance with the terminology adopted in reflectometry, the recording conditions specified in the diagrams correspond to rotation of the sample surface through a negative angle θ and detector scanning over the scale 2θ. In view of the fact that scanning was carried out in a limited angular range, with the direct beam detected as an angular reference, it is more convenient to plot on the abscissa the current scattering angle ψ, which is measured from the primary beam (ψ = 0) in the direction of the surface's normal.

The peaks observed on the right of the wing of the incident beam are caused by the refracted radiation. In accordance with expressions (6) and (8) obtained above, with increasing grazing angle θ_1, the angular shift θ_3 of the refracted beam with respect to the incident one decreases, and its intensity rises (see curves *1–3* for the wave CuK_α in Fig. 5a). For the radiation of shorter wavelength and the same angles θ_1, the angular shift θ_3 decreases (see Fig. 5b) and the ratio of intensities measured for the refracted and incident beams at the CuK_β line is larger than for the CuK_α line in accordance with (8).

The angular diagrams of intensity for the CuK_α line and the incidence of radiation onto the outer surface of a Ge–Si/Si sample arranged in position *B* (see Fig. 4) are shown in Fig. 6. The average period of the structure and the width of the Ge layer were equal to 22 and 0.7 nm, respectively, and the volume-averaged concen-

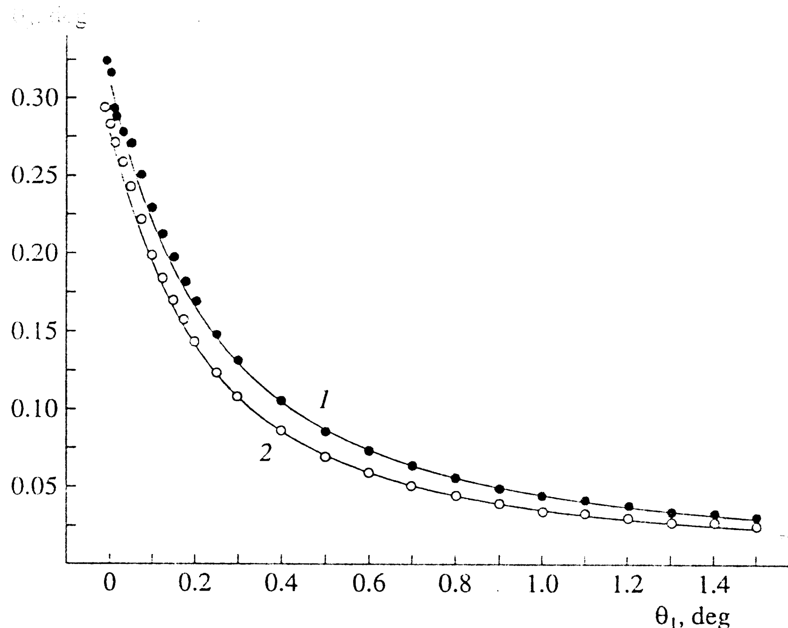

Fig. 7. Dependences of the deviation angle θ_3 on the grazing angle θ_1 for the incidence from inside on the surface of a GaAs single crystal for the (*1*) CuK_α and (2) CuK_β lines. The calculated curves are shown by the solid lines.

tration of Ge was lower than 3%. A sharp change of intensity at the beginning of the curves on the left is caused by the incident beam. The position of the specular reflection curves corresponds to the angle $2\theta_1$. The change of the noise spread of points for $\psi = 0.16°$ on curve *2* is associated with a switch of the operating mode of an X-ray tube. The decrease of the level of specularly reflected radiation with respect to the calculated value is due to partial stopping of the reflected flux by the screen *2*, which is drawn to the sample surface by the minimum possible distance.

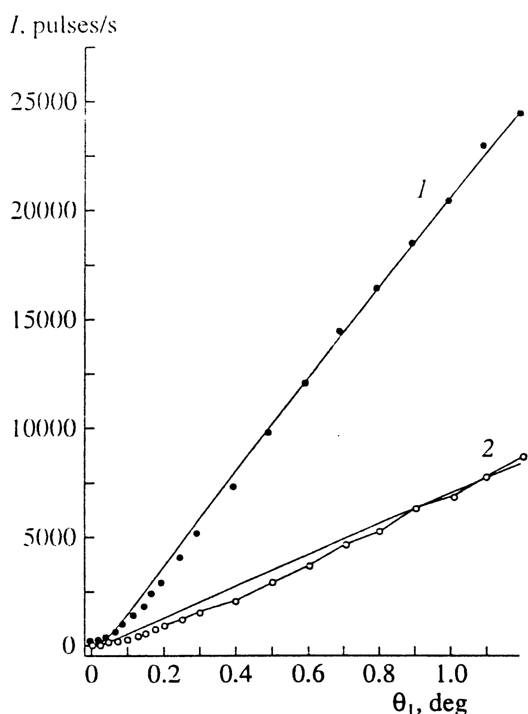

Fig. 8. Dependences of the refracted-radiation intensity on the grazing angle θ_1 for the incidence from inside on the surface of a GaAs single crystal for the (*1*) CuK_α and (2) CuK_β lines. The calculated curves are shown by the solid lines.

Note that the data in Figs. 5 and 6 are presented without correction for the spread function, and the true half-width of the peaks of refracted radiation is noticeably smaller. In this case, a noticeable broadening of the peaks under recording conditions chosen in the experiments was not observed because of the small size of the surface illuminated from the inside. Thus the character and form of the experimental dependences are in agreement with the expressions obtained above within the framework of geometrical optics.

For a qualitative verification of the validity of expressions (6) and (8), for the angular shift θ_3, we measured on a GaAs sample the dependences $\theta_3(\theta_1)$ and $I_t(\theta_1)$ in the range of θ_1 from 0° to 1.2°. The angular coordinates of the peaks and the integrated intensity under the peak of reflected radiation were determined upon subtraction of the wing of scattered radiation whose angular distribution was almost independent of θ_1 in the angular range under study. The experimental points obtained for the CuK_α and CuK_β lines are shown in Figs. 7 and 8, where they are superimposed on the calculated curves. The angular positions of the peaks of refracted radiation for the CuK_α and CuK_β lines nearly ideally fall on the curves calculated for GaAs. This means that when studying a sample with unknown composition or structure, the quantity δ and the elec-

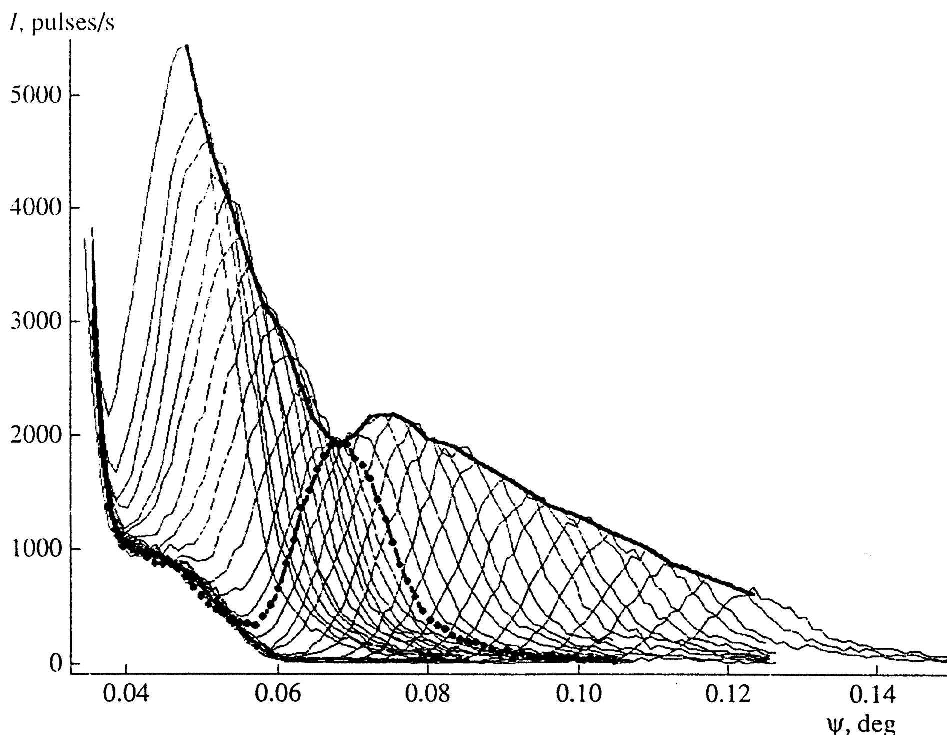

Fig. 9. Dependences of the refracted-radiation intensity on the grazing angle θ_1 for the CuK_α radiation traveling through a layered $Ge_{0.25}Si_{0.75}$–Si/Si heterostructure (seven pairs of layers with a calculated period of 14 nm).

tron density related to it can be determined with high accuracy from the angular position of the peak of refracted radiation. The deviation from a plane on a cleaved sample face along the boundary of intersection with a polished surface can have an effect on attenuation on a material and cause a noticeable deviation of the experimental dependence $I(\theta_1)$ from the calculated one. Because of this, in the general case the quantity β and the quantity μ linearly related to it, which are calculated from the data presented in Fig. 8, have a lower accuracy.

If a thin film is evaporated onto the sample surface or a layered heterostructure is grown on it, the radiation entering through a side face travels in a sample through two or more interfaces, and the reflectivity is determined by the interference of waves and reflections from all the boundaries. Direct recording of $I(\theta_1)$ is made difficult by the fact that a sample and a receiving detector slit should be moved in the regime $\theta_1 - \theta_3$, with θ_3 being nonlinearly dependent on θ_1. One can solve the given problem by way of recording a series of angular scattering diagrams $I(\psi)$ for a set of fixed angular positions of a sample. By way of example, we show in Fig. 9 a series of such diagrams for a $Ge_{0.25}Si_{0.75}$–Si/Si sample set in position *A*. Seven pairs of $Ge_{0.25}Si_{0.75}$ and Si layers were grown by molecular-beam epitaxy on a Si substrate. The deviation of the period from the average value by 5–10% was allowed, and the thicknesses of $Ge_{0.25}Si_{0.75}$ and Si layers were in proportion 1 : 2. The initial value of the grazing angle θ_1 was equal to 0.15°, and its value upon measurement of $I(\psi)$ increased by 0.01°. For $\theta_1 = 0.32°$ (see the curve with singled-out experimental points), one can clearly see on the envelope of the series of experimental curves a dip corresponding to the first Bragg reflection order for the period $d \approx 14$ nm.

CONCLUSION

The results obtained by us show that the version of X-ray refractometry proposed here, which is carried out through a side-cleaved surface, is an effective method for determining the real and imaginary parts of the refractive index and related parameters (the density, the material composition). The method is universal; i.e., one can use it for the analysis of any kind of solids independently of their structure. The only condition is the presence of an optically smooth plane face of width ≥ 0.1 mm that forms, with a side surface, an angle $\sim\pi/2$.

Refractometry may be of particular interest for the study of samples in the case where part of their surface is occupied by a device structure, conductor strips, etched grooves, etc., i.e., when the application of the standard X-ray reflectometry is impracticable or gives ambiguous results.

When studying multilayer structures, one can find, on the angular dependence of refracted radiation, minima corresponding to different Bragg reflection orders.

Since radiation is transmitted into a sample through a side cleaved face and leaves it almost without refraction, this feature in combination with the reflectometry data makes it possible to obtain a more complete and reliable set of information on a multilayer structure.

ACKNOWLEDGMENTS

We are grateful to M. Rzaev who placed heterostructure samples at our disposal.

REFERENCES

1. Tour'yanski, A.G., Vinogradov, A.V., and Pirshin, I.V., *Prib. Tekh. Eksp.*, 1999, no. 1, p. 105.
2. Hartley, C.C., *Phys. Rev.*, 1924, vol. 24, p. 486.
3. Larsson, A., Siegbahn, M., and Waller, T., *Phys. Rev.*, 1925, vol. 25, p. 235.
4. Davis, B. and Slack, C.M., *Phys. Rev.*, 1925, vol. 25, p. 881.
5. Davis, B. and Slack, C.M., *Phys. Rev.*, 1926, vol. 27, p. 18.
6. Blokhin, M.A., *Fizika rentgenovskikh luchei* (X-ray Physics), Moscow: GITTL, 1957.
7. Vinogradov, A.V., Brytov, I.A., Grudskii, A.Ya., *et al.*, *Zerkal'naya rentgenovskaya optika* (Mirror X-Ray Optics), Leningrad: Mashinostroenie, 1989.
8. Snigirev, A., Kohn, V., Snigireva, I., and Lengeler, B., *Nature* (London), 1996, vol. 384, p. 49.
9. Ingal, V.N. and Belyavskaya, E.A., Abstracts of Papers, *Natsional'naya konferentsiya po primeneniyu rentgenovskogo, sinkhrotronnogo izluchenii, neitronov i elektronov dlya issledovaniya materialov* (National Conf. on Application of X- and Synchrotron Radiation, Neutrons, and Electrons for Studies of Materials), Dubna, 1997, p. 363.
10. Bushuev, V.A. and Kone, A., *Poverkhnost*, 1998, no. 10, p. 5.
11. Born, M. and Wolf, E., *Principles of Optics*, London: Pergamon, 1964. Translated under the title *Osnovy optiki*, Moscow: Nauka, 1973.
12. Tour'yanski, A.G. and Pirshin, I.V., *Prib. Tekh. Eksp.*, 1998, no. 5, p. 118.